Simulation of satellite chlorophyll-a measures using *in situ* data

Lilian Anne Krug [1]

[1] Centre of Excellence in Observational Oceanography – Nippon Foundation and Partnership for Observations of the Global Ocean (NF-POGO), Bermuda Institute of Ocean Sciences.
17, Biological Station, Ferry Reach, St. George's GE 01, Bermuda
licakrug@yahoo.com.br

Abstract. Ocean colour orbital sensors can collect information of the first quarter of the photic zone depth. This study proposed to calculate the chlorophyll-a concentration for this penetration depth and to compare it with the satellite product. The photic and penetration depths at the Bermuda Atlantic Time Series (BATS) station were obtained from the diffuse light attenuation profiles. These, in turn, were based on the inherent optical properties, absorption and scattering, estimated from *in situ* chlorophyll-a measurements. The chlorophyll-a concentrations were calculated for the penetration depths of 440 nm, 550 nm and of the entire photosynthetic active region (PAR – 400-700 nm). The results show good linear correlations between the satellite product and penetration depth chlorophyll-a concentrations ($R^2 > 0.6$). Both monthly and weekly SeaWiFS products underestimate *in situ* chlorophyll-a when its concentration is higher than 0.15 mg m^{-3}, probably due to the algorithm scheme of chlorophyll-a retrieval. Ten-year time series were constructed to analyze the seasonal patterns. The photic and penetration depths, as the subsurface chlorophyll-a maximum, tend to become shallower at the beginning of spring season (February to April) and deepen in summer season (June to July). This pattern might be associated with phytoplankton blooms and the mixed layer depth (MLD) seasonality.

Palavras-chave: ocean colour, inherent optical properties, penetration depth, cor do oceano, propriedades ópticas inerentes, profundidade de penetração.

1. Introduction

In the radiometric data received by an orbital optical scanner, the amount of information on water column relevant to ocean colour studies is impressively low. This occurs because the sunlight beam is reduced in both directions, down and upwards, both while crossing the atmosphere and within the ocean.

The attenuation of the light in the water column depends on its inherent optical properties (IOPs), the absorption and scattering of the water molecules, particulate and dissolved constituents (Kampel and Novo, 2005). In open waters the phytoplankton may be considerate the main player on variations of the optical properties, the IOPs, and therefore the light attenuation, can be expressed as a function of the concentration of its main pigment, the chlorophyll-a (Sathyendranath et al., 2001).

Due the scarce presence of particulate and dissolved materials in oceanic waters the photic zone depth – the depth where the light is attenuated to 1% of its intensity at the surface – is larger than in coastal waters. Still, satellites can 'see' only the first portion of the photic zone, the penetration depth, and returns a weighted average value over this layer (Sathyendranath and Platt, 1989).

The objective of this study is to compare chlorophyll-a concentration estimated by the satellite with a simulated satellite data, where the concentration at an inferred penetration depth was estimated based on *in situ* chlorophyll-a profiles. The seasonal variability of the chlorophyll-a and the photic and penetration depths are analyzed in a ten-year time series.

2. Methodology

2.1. Photic and penetration depths

In order to obtain the chlorophyll-a concentration at the penetration depth (z_{pe}) first is necessary to estimate the photic depth (z_p). The photic depth is defined as that depth where irradiance (E) is reduced to 1% of its value at the surface (Platt et al., 1994), i.e. $E_{(\lambda,z_p)} = 0.01E_{(\lambda,surface)}$. The irradiance loss at each depth can be determined as:

$$E_{(\lambda,z_n)} = E_{(\lambda,z_{n-1})} e^{-K_{(\lambda,z_n)}(z_n - z_{n-1})} \quad (1)$$

where $K_{(\lambda,Zn)}$ is the light attenuation coefficient at depth n and wavelength λ.

The attenuation coefficient (K) has the dimensions of length (typically, m^{-1}), and the quantity K^{-1} is called the optical depth of the water. The photic zone layer has approximately 4.6 optical depths (Platt and Sathyendranath, 2010):

$$z_p = {}^{1}\!/\!_{K} \log_e \left(\frac{E_{(\lambda,surface)}}{E_{(\lambda,z)}} \right) = {}^{1}\!/\!_{K} \log_e 100 \approx \frac{4.6}{K} \quad (2)$$

According to Gordon and McCluney (1975), 90% of the upwelling water radiance at sea surface belongs to the first optical depth, denominated penetration depth. Based on Equation 2, this study assumes that the penetration depth is equivalent to the first 25% of the photic depth ($z_{pe} = {}^{z_p}\!/\!_{4}$).

2.2. Light attenuation, absorption and backscattering coefficients

The light attenuation coefficient can be stated as a function of the inherent optical properties of the water column, the absorption and backscattering (Sathyendranath et al., 2001):

$$K_{(\lambda,z_n)} = \frac{(a_{(\lambda,z_n)} + b_{b_{(\lambda,z_n)}})}{\mu_d} \quad (3)$$

where $a_{(\lambda,zn)}$ is the absorption coefficient for wavelength λ at depth n, $b_{b(\lambda,zn)}$ is the backscattering coefficient for wavelength λ at depth n and μ_d is the mean cosine for downwelling light.

The absorption coefficient is the joined effect of the absorption of the different elements present at the water column (Sathyendranath et al., 2001):

$$a_{(\lambda,z_n)} = a_w(\lambda) + a_y(\lambda) + a_p \quad (4)$$

where a_w is the absorption coefficient of pure water at wavelength λ, a_y is the absorption coefficient of the yellow substance and a_p is the particulate material absorption coefficient. Since this study area is located in an open ocean region, a_p is assumed to be dominated by phytoplankton absorption.

While $a_w(\lambda)$ is a single wavelength-dependent value (Table 3 in Pope and Fry, 1997), the other equation components are calculated as (Sathyendranath et al., 2001; Devred et al., 2006):

$$a_{y(\lambda)} = a_{y(440nm)} \exp^{-0.014(\lambda - 440)} \quad (4.1)$$

where $a_y(440\ nm)$ is the absorption coefficient of the yellow absorption at 440 nm and co-varies with the phytoplankton absorption at the same wavelength ($a_{p(440\ nm)}$):

$$a_{y(440nm)} = 0.3 a_{p(440nm)} \quad (4.1.1)$$

The phytoplankton absorption coefficient was modelled by Sathyendranath et al. (2001) and improved in Devred et al. (2006). It considers specific absorption coefficients for two different populations of phytoplankton, distinguished by size and harvest efficiency. It is

assumed that the total chlorophyll-a concentration (C) is dominated by population 1 chlorophyll-a (C_1) until C reaches a certain threshold. Higher than this concentration, population 2 chlorophyll-a turns the dominant component, such that:

$$a_{p(\lambda)} = C_1^m \left[a_{1(\lambda)}^* - a_{2(\lambda)}^* \right] \left[1 - \exp(-\frac{1}{C_1^m} C) \right] + a_{2(\lambda)}^* C \quad (4.2)$$

where, C_1^m is the maximum value of C_1, $a_{1(\lambda)}^*$ and $a_{2(\lambda)}^*$ are specific absorption coefficient of populations 1 and 2 at wavelength λ and C is total chlorophyll. From in situ data collected in several cruises, Devred et al. (2006) computed the parameters $C_1^m, a_{1(\lambda)}^*$ and $a_{2(\lambda)}^*$ (Tables 2 and 3 in Devred et al., 2006).

For the backscattering coefficient at wavelength λ and depth n, Sathyendranath et al. (2001) present:

$$b_{b(\lambda,z_n)} = b_{bw}(\lambda) + \tilde{b}_{bp}\, b_p(\lambda) \quad (5)$$

where $b_{bw}(\lambda)$ is the backscattering coefficient of pure water at wavelength λ (Equation 5.1), $\tilde{b}_{bp}$ is the ratio of backscattering and total scattering coefficient by particles ($\tilde{b}_{bp} = b_{bp(\lambda)} / b_{p(\lambda)}$) and $b_p(\lambda)$ is the scattering coefficients of particles (Equation 5.2).

Based on Morel (1974), due to molecules symmetry the backscattering coefficient of pure water (b_{bw}) is 50% of total scattering (b_w) and is calculated as:

$$b_{bw(\lambda)} = 0.5 b_{w(500nm)} \left(\frac{\lambda}{500} \right)^{-4.3} \quad (5.1)$$

where $b_{w(500\ nm)}$ is the scattering coefficient of pure water at 500 nm: 0.00288 m^{-1}.

The scattering coefficient of particles is also a function of wavelength, defined as (Loisel and Morel, 1998; Sathyendranath et al., 2001):

$$b_{p(\lambda)} = b_{p(660nm)} \left(\frac{660}{\lambda} \right)^{-\log_{10} C} \quad (5.2)$$

where C stands for chlorophyll-a concentration and $b_{p(660nm)}$ is the scattering coefficient of particles at 660 nm:

$$b_{p(660)} = 0.407 C^{0.795} \quad (5.2.1)$$

Ulloa et al. (1994) and Sathyendranath et al. (2001) define the backscattering/scattering ratio for particles as:

$$\tilde{b}_{b(\lambda)} = 0.01(0.78 - 0.42 \log_{10} C) \quad (5.3)$$

2.3. Chlorophyll-a at the penetration depth

With the light attenuation coefficient (K) profiles calculated, the photic and penetration depths are estimated (Equations 1 and 2) allowing the calculation of the chlorophyll-a concentration at the penetration depth (C_{pe}). The equation considers that shallower the water parcel, higher its contribution to the radiance at surface:

$$C_{pe(\lambda)} = \frac{\int_0^{z_{pe}(\lambda)} C_z f(z) dz}{\int_0^{z_{pe}(\lambda)} f(z) dz} \quad (6)$$

where $z_{pe}(\lambda)$ is the penetration depth (m), C_z the chlorophyll concentration at depth z and f(z) is:

$$f(z) = \exp^{-2} \int_0^{z_{pe}} K(z').dz' \quad (6.1)$$

The chlorophyll-a concentrations were calculated for the penetration depths of 440 nm, 550 nm and of the entire photosynthetic active region (PAR – 400-700 nm).

2.4. *In situ* chlorophyll-a concentration

The Bermuda Atlantic Time Series (BATS) is located in the western North Atlantic subtropical gyre (Michaels et al., 1994; Steinberg et al., 2001). Since 1988, the Bermuda Institute of Ocean Sciences (BIOS) conduct cruises on a biweekly to monthly basis to sample phytoplankton pigments among others physical, chemical and biological data at BATS station (31º10' N - 64º10' W). Sampling methodology is described in Steinberg et al. (2001).

A total of 111 profiles (0 m – 250 m) of *in situ* chlorophyll-a concentration was obtained from the BATS database (http://www.bats.bios.edu) constituting a ten-years time series (1997-2007). Typically, 12 samples at different depths cover the first 250 m of the water column. Here, these values were interpolated to reconstruct profiles with 1 m interval.

2.5. Satellite chlorophyll-a concentration

Averaged concentrations of chlorophyll-a at BATS location were obtained from monthly and weekly 9 km-resolution products of SeaWiFS for the correspondent period of the *in situ* chlorophyll-a time series. The data was acquired from the GES-DISC Interactive Online Visualization And aNalysis Infrastructure (Giovanni) as part of the NASA's Goddard Earth Sciences (GES) Data and Information Services Centre (http://reason.gsfc.nasa.gov/OPS/Giovanni/ocean.seawifs.shtml)

The SeaWiFS chlorophyll-a concentrations are estimated with a fourth order polynomial equation, where the algorithm OC4v4 makes use of different ratios among blue and green bands (O'Reilly et al., 2000). This algorithm was based on empirical relations of *in situ* water leaving radiance and chlorophyll-a concentrations in a variety of ocean provinces which have different optical properties. As older versions, OC4v4 has a considerate good performance in open ocean waters with chlorophyll-a concentrations between 0.03 mg m^{-3} to 1 mg m^{-3} (O'Reilly et al., 2000).

3. Results and discussion

3.1. *In situ* chlorophyll-a concentration at BATS

For the 10-years time series, BATS average chlorophyll-a concentration at the first 250 m is 0.1 mg m^{-3} with a maximum of 0.7 mg m^{-3} (Figure 1), characteristic of low chlorophyll waters.

Elevated concentrations reach the surface near April and vary from 60 m to 110 m throughout the rest of the year (Figure 1 and 2). According to Longhurst and Harrison (1989), the maximum chlorophyll-a concentration occurs near surface during phytoplankton bloom

and near the photic depth in stable conditions. At this elevated depth, light intensity is low and the phytoplankton has to increase its cellular chlorophyll content in order to maintain efficiency. This subsurface chlorophyll-a maximum (SCM) presented an average concentration of 0.3 mg m^{-3}, with minimum and maximum of 0.03 mg m^{-3} and 0.7 mg m^{-3}, respectively.

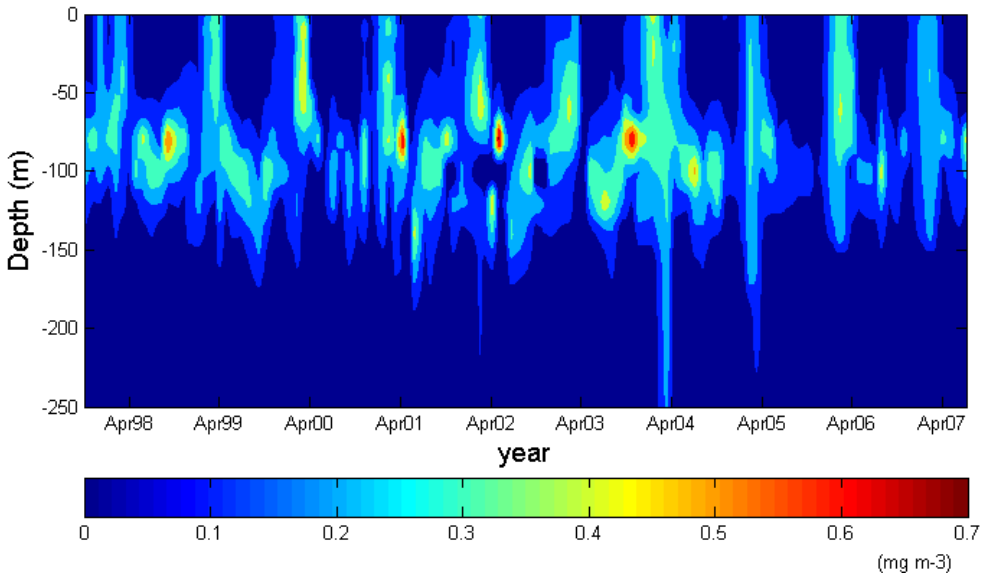

Figure 3 - Chlorophyll-a concentration at Bermuda Atlantic Time Series

3.2. Photic and penetration depths at BATS

The photic depths presented higher depth for the lower wavelength, 440 nm, and the shallower depths for the green wavelength (550 nm), approximately 160 m and 60 m respectively (Figure 4). The photic depth for the photosynthetic active region (PAR), which constitutes the entire visible and near infrared spectra (400 to 700 nm) had an intermediary average of 110 m. The approximate average for the penetration depth (z_{pe}) were 40 m, 15 m and 27 m for 440 nm, 550 nm and PAR respectively.

The time series showed an oscillating behaviour for z_p and z_{pe} at 440 nm and PAR wavelengths similar to the subsurface chlorophyll-a maximum (Figure 4). The shoaling at z_p, z_{pe} at 440 nm and PAR and SCM occurs at the beginning of spring season (February to April) and deepening in summer (June, July). This pattern might be associated with the mixed layer depth (MLD) seasonality. In winter, the low temperatures and strong wind conditions deepen the vertical mixing, bringing nutrient-rich waters from deep layers to the photic zone. In beginning of spring, with both nutrients and light available, the rate of phytoplankton growth increases causing the spring blooms. An increase in phytoplankton elevates the particulate and dissolved matter (from decomposing material) concentrations, increasing the attenuation of light at surface and consequently reducing the photic depth.

In summer the higher light availability and the increased surface temperature generate a pronounced, shallower thermocline turning the MLD thinner and ceasing the renewal of nutrients from deep waters. This situation inhibits the phytoplankton growth, reducing the particulate and dissolved matter.

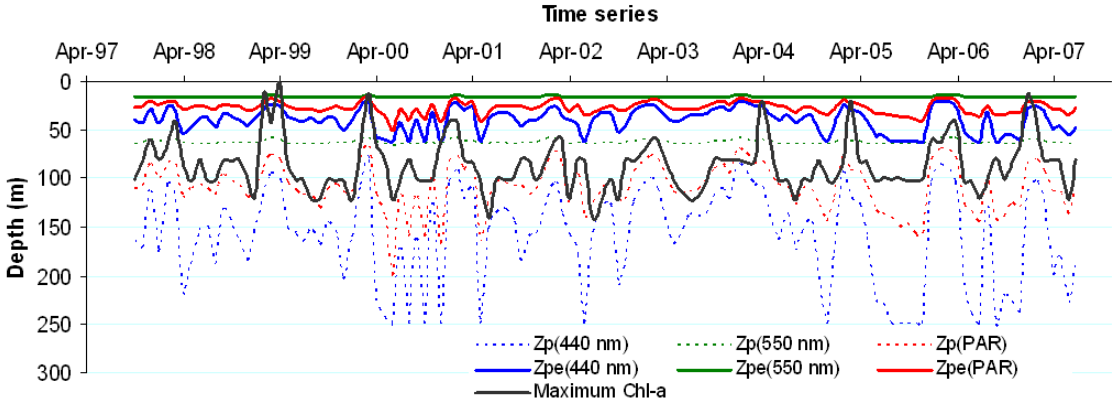

Figure 4 - Time series of photic depth (Zp), penetration depth (Zpe) and deep maximum chlorophyll-a at BATS station for different wavelengths.

3.3. Comparison between *in situ* and satellite chlorophyll-a

The temporal variation of *in situ* and satellite chlorophyll-a concentrations was very similar, but with different magnitudes (Figure 5). From October 1997 to July 2007, chlorophyll-a concentrations extracted of the monthly and weekly SeaWiFS products vary between 0.04 mg m^{-3} to 0.21 mg m^{-3}, while chlorophyll-a at the penetration depth for the 440 nm and 550 nm wavelengths and PAR minimum and maximum were 0.01 and 0.59 mg m^{-3}, respectively.

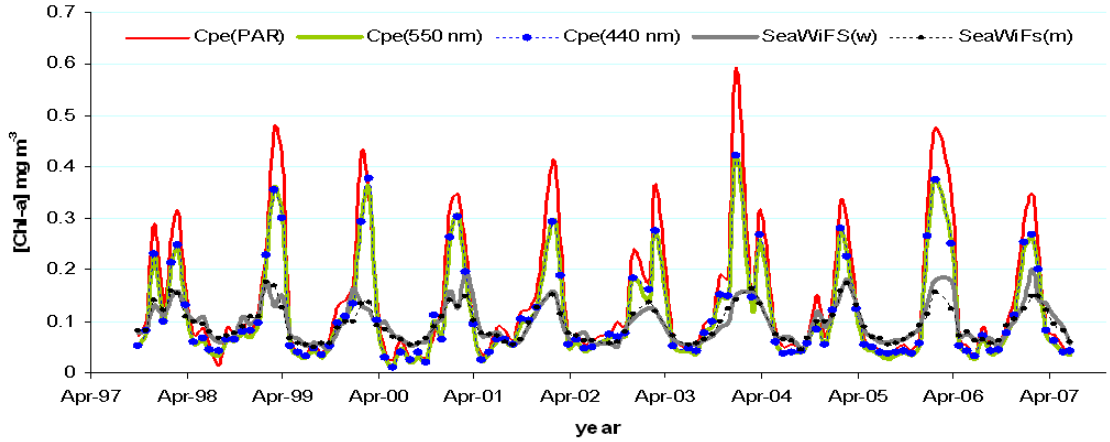

Figure 5 – Chlorophyll-a concentrations at 440 nm, 550 nm and PAR penetration depths ($C_{pe(440\ nm)}$, $C_{pe(550\ nm)}$ and $C_{pe(PAR)}$) and monthly (m) and weekly (w) SeaWiFS products.

Although $z_{pe(440\ nm)}$ and $z_{pe(550\ nm)}$ had an average difference of 25 m (Figure 4) their chlorophyll-a content was practically identical: an average of 0.11 mg m^{-3} for both (Figure 5). SeaWiFS products also were very similar with average concentration values of 0.09 mg m^{-3} (monthly) and 0.10 mg m^{-3} (weekly).

The difference between SeaWiFS and *in situ* chlorophyll-a concentrations may be a result of the algorithm that generates the satellite product. O'Reilly et al. (2000) describe that the relation between *in situ* upwelling radiance at surface and chlorophyll-a concentration is the basis for the polynomial equation OC4v4 uses to prepare the data.

The disparity between both acquisitions (satellite and *in situ*) was more discernible in higher concentrations (> 0.15 mg m^{-3} – Figure 5). The closeness of SCM and penetration depth for this time periods (Figure 4) may indicate an elevation on chlorophyll-a concentration in depths neglected by the algorithm. When plotted, the correlation between

these datasets evidenced good linear relations (Table 1) and this underestimation of concentrations above ~0.15 mg m^{-3} by the SeaWiFS products, here represented by Monthly SeaWiFS data and $z_{pe(440\ nm)}$ (Figure 6).

Table 1 – Correlation coefficients (R^2) between the chlorophyll-a concentrations at the penetration depths and obtained from SeaWiFS products.

	SeaWiFS product	
In situ	Monthly	Weekly
$C_{pe(440\ nm)}$	0.76	0.64
$C_{pe(550\ nm)}$	0.69	0.69
$C_{pe(PAR)}$	0.66	0.63

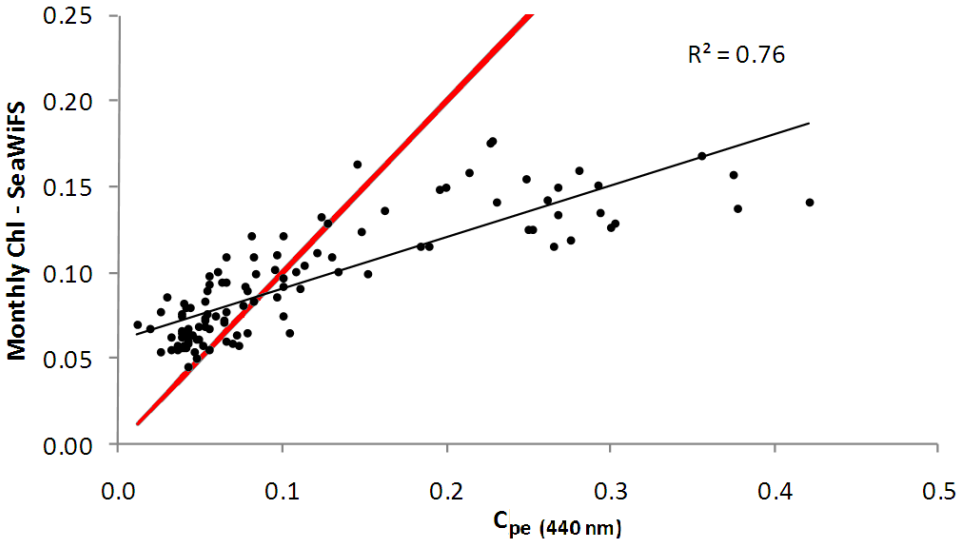

Figure 6 – Relation between chlorophyll-a concentration for the estimated penetration depth at 440 nm and SeaWiFS monthly average. Trend and identity lines in black and red, respectively.

The results presented here still are object of study. The next steps include detailed study of the uncertainties originated by the assumptions and analysis of the interannual variations observed. The relation to environmental variables, such as sea surface temperatures and eddies, and influence of major events, like hurricanes and ENSO will be investigated.

4. Conclusions

In theory the depth satellites are able to sense is fairly variable depending on wavelength and time of the year. The depth where chlorophyll-a has its maximum concentration is much higher than this penetration depth throughout most part of the year, excepting periods of bloom, where chlorophyll-a increases near surface.

Satellite-derived chlorophyll-a concentrations were well correlated with the chlorophyll-a present at the penetration depth, but underestimate it when the concentrations are high. This is probably a result of the algorithm used for the product generation.

It is important to highlight that the usefulness of remote sensing lies in the synoptic coverage it provides, the accuracy depends on careful algorithm design and the interpretation is enhanced with *in situ* observations, reinforcing the value of long time series such as BATS.

5. Acknowledgments

The author wishes to express her gratitude to Dr. Trevor Platt and Dr. Shubha Sathyendranath for the exciting and challenging exercise and the generous guidance to accomplish it. To Dr. George White III, Dr. Li Zhai and Dr. Heather Bouman for sharing their knowledge. To the Bermuda Institute of Ocean Sciences (BIOS), the

Nippon Foundation (NF) and the Partnership for Observations of the Global Ocean (POGO) for support the Observational Oceanography training at BIOS.

6. References

Devred, E.; Sathyendranath, S.; Stuart, V.; Maass, H.; Ulloa, O.; Platt, T. A two-component model of phytoplankton absorption in the open ocean: Theory and applications. **Journal of Geophysical Research,** v. 111, n. C03011, p.1-11, 2006.

Gordon, H. R; McCluney, W. R. Estimation of the depth of sunlight penetration in the sea for remote sensing. **Applied Optics**, v. 14, n. 2, p. 413-416, 1975.

Kampel, M. e Novo, E. M. L. O sensoriamento remoto da cor da água. In: Souza, R.B. (org**.). Oceanografia por satélites**. São Paulo: Oficina de Textos, p. 179-196, 2005.

Loisel, H.; Morel, A. Light scattering and chlorophyll concentration in case 1 waters: a reexamination. **Limnology and Oceanography**, v. 43, n. 5, p. 847–858, 1998.

Longhurst, A. R.; Harrison, W. G. The biological pump: Profiles of plankton production and consumption in the upper ocean. **Progress in Oceanography**, v. 22, n. 1, p. 47 - 123, 1989.

Michaels, A.F.; Knap, A.H.; Dow, R.L.; Gundersen, K.; Johnson, R.J.; Sorensen, J.; Close, A.; Knauer, G.A.; Lohrenz, S.E.; Asper, V.A.; Tuel, M.; Bidigare, R.R.Seasonal patterns of biogeochemistry at the US JGOFS Bermuda Atlantic Time-series Study side. **Deep-Sea Research I**, v. 41, n. 7, p. 1013–1038, 1994.

Morel, A. Optical properties of pure seawater. In: Jerlov, N. G.; Nielsen, E. S. (org) **Optical Aspects of Oceanography**, New York: Academic, p. 1-24, 1974.

O'Reilly, J. E.; Maritorena, S.; Siegel, D.; O'Brien, M. C.; Toole, D.; Mitchell, B. G.; Kahru, M.; Chavez, F. P.; Strutton, P.; Cota, G.; Hooker, S. B.; McClain, C. R.; Carder, K. L.; Müller-Karger, F.; Harding, L.; Magnuson, A.; Phinney, D.; Moore, G. F.; Aiken, J.; Arrigo, K. R.; Letelier, R.; Culver, M. Ocean color chlorophyll a algorithms for SeaWiFS, OC2, and OC4: Version 4. In: Hooker, S.B.; Firestone, E.R. (org). **SeaWiFS Postlaunch Technical Report Series, Volume 11, SeaWiFS Postlaunch Calibration and Validation Analyses, Part 3.** Maryland: NASA, Goddard Space Flight Center, 2000, p. 9-23.

Platt, T.; Sathyendranath, S. Modelling primary production – IV. Daily primary production of the water column: General introduction. p. 27 – 35. Available at: < http://www.geosafari.org/kochi/Forms/PPMOMNI.pdf>. Accessed in: 19.nov.2010.

Platt, T.; Sathyendranath, S.; White, G.; Ravindran, P. Attenuation of visible light by phytoplankton in a vertically structured ocean: solutions and applications. **Journal of Plankton Research**, v. 16, n. 11, p. 1461-1487, 1994.

Pope, R. M.; Fry, E. S., Absorption spectrum (380–700 nm) of pure water: II. Integrating cavity measurements. **Applied Optics**, v. 36, n. 33, p. 8710–8723, 1997.

Sathyendranath, S.; Platt, T. Remote sensing of ocean chlorophyll: consequence of non uniform pigment profile. **Applied Optics**, v. 28, n. 3, p. 490-495, 1989.

Sathyendranath, S.; Cota, G.; Stuart, V.; Maass, H.; Platt, T. Remote sensing of phytoplankton pigments: a comparison of empirical and theoretical approaches. **International Journal of Remote Sensing**, v. 22, n. 2-3, p. 249–273, 2001.

Steinberg, D.K.; Carlson, C.A.; Bates, N.R.; Johnson, R.J.; Michaels, A.F.; Knap, A. Overview of the US JGOFS Bermuda Atlantic Time-series Study (BATS): a decade-scale look at ocean biology and biogeochemistry. **Deep-Sea Research II**, v. 48, p. 1405–1448, 2001.

Ulloa, O.; Sathyendranath, S.; Platt, T. Effect of the particle–size distribution on the backscattering ratio in seawater. **Applied Optics,** v. 33, n. 30, p. 7070–7077, 1994.